Structural Features Associated With the Development and Progression of RORA Secondary to Maternally Inherited Diabetes and Deafness

PHILIPP L. MÜLLER, PETER MALOCA, ANDREW WEBSTER, CATHERINE EGAN, AND ADNAN TUFAIL

• PURPOSE: To investigate the development and progression of retinal pigment epithelial and outer retinal atrophy (RORA) secondary to maternally inherited diabetes and deafness (MIDD).

• DESIGN: Retrospective observational case series.

• METHODS: Thirty-six eyes of 18 patients (age range, 22.4-71.6 years) with genetically proven MIDD and serial optical coherence tomography (OCT) images were included. As proposed reference standard to diagnose and stage atrophy, OCT images were longitudinally evaluated and analyzed for presence and precursors of RORA. RORA was defined as an area of (1) hypertransmission, (2) disruption of the retinal pigment epithelium, (3) photoreceptor degeneration, and (4) absence of other signs of a retinal pigment epithelial tear.

• RESULTS: The majority of patients revealed areas of RORA in a circular area around the fovea of between 5° and 15° eccentricity. Over the observation time (range, 0.5-8.5 years), evidence for a consistent sequence of OCT features from earlier disease stages to the end stage of RORA could be found, starting with loss of ellipsoid zone and subretinal deposits, followed by loss of external limiting membrane and loss of retinal pigment epithelium with hypertransmission of OCT signal into the choroid, and leading to loss of the outer nuclear layer bordered by hyporeflective wedges. Outer retinal tabulations seemed to develop in regions of coalescent areas of RORA.

• CONCLUSIONS: The development and progression of RORA could be tracked in MIDD patients using OCT images, allowing potential definition of novel surrogate markers. Similarities to OCT features in age-related macular degeneration, where mitochondrial dysfunction has been implicated in the pathogenesis, support wide-ranging benefits from proof-of-concept studies in MIDD. (Am J Ophthalmol 2020;218:136–147. © 2020 Elsevier Inc. All rights reserved.)

AJO.com Supplemental Material available at AJO.com.

Accepted for publication May 14, 2020.

From the Moorfields Eye Hospital NHS Foundation Trust (P.L.M., P.M., A.W., C.E., A.T.), London, UK; Department of Ophthalmology, University of Bonn (P.L.M.); Center for Rare Diseases, University of Bonn (P.L.M.), Bonn, Germany; Department of Ophthalmology, University of Basel (P.M.); Institute of Molecular and Clinical Ophthalmology Basel (P.M.), Basel, Switzerland; and Institute of Ophthalmology, University College London (A.W.), London, UK

Inquiries to Adnan Tufail, Moorfields Eye Hospital NHS Foundation Trust, 162 City Rd, London EC1V 2PD, United Kingdom; e-mail: adnan.tufail@nhs.net

INTRODUCTION

MATERNALLY INHERITED DIABETES AND DEAFNESS (MIDD, Online Mendelian Inheritance in Man # 520000) is a mitochondriopathy, which was first described in 1992,[1] and is primarily caused by mutation in the *Mitochondrially Encoded TRNA Leucine 1* (*MTTL1*) gene at position 3243.[2,3] The majority (50%-85%) of patients reveal a pattern like dystrophy and/or retinal pigment epithelial and outer retinal atrophy (RORA) with phenotypic similarities to age-related macular degeneration (AMD).[4,5]

New promising therapeutic strategies focusing on mitochondrial dysfunction have recently been presented.[6] Mitochondrial dysfunction also has been implicated in the pathogenesis of multifactorial disease, such as AMD, which is the leading cause of legal blindness in the industrialized world.[7] Given the fact that multifactorial diseases are driven by heterogeneous risk factors, the effect of these specific strategies can more effectively be evaluated in a pure mitochondriopathy. In this context, MIDD is a model disease for ocular phenotypes caused by mitochondrial dysfunction.

To accelerate clinical testing, meaningful, validated clinical endpoints need to be developed. Most interventional trials currently rely on the progression of RORA, which depicts the end stage of many retinal diseases and an accepted endpoint by regulators for studies of atrophic AMD (called "geographic atrophy" [GA]).[8,9] However, the most effective upcoming therapeutic approach might be directed to earlier disease stages.[10] Therefore, ideal surrogate markers should be easily captured, reflect the current disease severity, be predictive for long-term progression based on short-term changes, and identify early disease-

0002-9394/$36.00
https://doi.org/10.1016/j.ajo.2020.05.023

associated alterations ideally before the hitherto unknown point of no return.

A consensus of worldwide retinal specialists has recommended that optical coherence tomography (OCT) should be the primary imaging method to define RORA.[11] Earlier OCT alterations have been described and shown to be associated with the development of RORA in AMD, which have the potential to serve as surrogate markers for therapeutic approaches and even allow for automated analysis.[12] However, there has not been a similar investigation of OCT features in patients with MIDD. Therefore, we systematically and longitudinally investigated OCT scans in MIDD. We aimed to define features that might be relevant to the development and progression of RORA in this specific mitochondrial disease. The results of this pilot study may lead to further investigations that analyze the reliability of these parameters and accuracy as predictive factors.

TABLE. Demographic, functional and imaging parameters of included subjects

Parameter	Subjects
Number of eyes (patients)	36 (18)
Sex, female/male	11/7
Age at baseline, y[a]	53.4 ± 11.6
Age of onset, y[a]	47.3 ± 8.4
Disease duration at baseline, y[a]	6.1 ± 6.2
Best-corrected visual acuity at baseline, logMAR[a]	0.19 ± 0.25
Presence of RORA at baseline, eyes (patients)	33 (17)
Size of RORA at baseline, mm^2[a]	15.9 ± 20.1
Focality of RORA at baseline[a]	2.8 ± 1.8
Follow-up time, y[a]	4.6 ± 2.8

logMAR, logarithm of the minimum angle of resolution.
[a]Values indicate mean ± standard deviation

METHODS

THIS RETROSPECTIVE OBSERVATIONAL CASE SERIES WAS performed at Moorfields Eye Hospital, London, United Kingdom. The study was in adherence with the Declaration of Helsinki. Approval by the local research governance committee from the Research and Development Department, and patients' informed consent was obtained for the study.

• **PATIENT SELECTION:** Eligible participants were identified by text search of electronic medical records from dedicated Medical Retina clinics of the study team at the Moorfields Eye Hospital, London, United Kingdom, between 2004 and 2019. The search terms were *maternally inherited diabetes and deafness*, *MIDD*, and *m.3243A>G*.

The inclusion criteria were defined as (1) presence of the m.3243A>G variant in the *MTTL1* gene, (2) a compatible phenotype consistent with the clinical diagnoses of MIDD, and (3) serial OCT scans with an interval of at least 6 months. Other macular pathology and/or OCT images inadequate to evaluate (eg, insufficient image quality) led to exclusion. If both eyes met the inclusion criteria, both were included.

• **IMAGING:** All participants underwent a complete ophthalmic examination including best-corrected visual acuity testing, slit-lamp examination, and indirect ophthalmoscopy in routine clinical settings. Before multimodal imaging, pupils were dilated. The imaging protocol included spectral-domain OCT (Spectralis HRA+OCT, Heidelberg Engineering, Heidelberg, Germany) and short-wavelength fundus autofluorescence (AF) imaging (488-nm excitation and 500-700-nm emission) using 2 different generations of a confocal scanning laser ophthalmoscopy system (HRA classic, HRA 2, or Spectralis HRA+OCT; Heidelberg Engineering) according to the availability at the study center at the time of visit. The image resolution was 512 × 512 pixels for the HRA classic, whereas HRA 2 and Spectralis HRA+OCT recorded images with 768 × 768 pixels (high-speed mode) or 1,536 × 1,536 pixels (high-resolution mode). Using the device-inbuilt tracking feature, up to 100 images (centered on the fovea) were automatically aligned and averaged to optimize the signal-to-noise ratio.

• **IMAGE ANALYSIS:** OCT scans were analyzed using the manufacturer's software (Heidelberg Eye Explorer; Heidelberg Engineering). In accordance with the previously described practice,[11] presence of RORA was defined as (1) a region of hypertransmission, (2) a zone of attenuation or disruption of the retinal pigment epithelium, (3) evidence of overlying photoreceptor degeneration, and (4) absence of scrolled retinal pigment epithelium or other signs of a retinal pigment epithelial tear. After defining the exact location of RORA, present and preceding OCT scans were investigated for alterations associated with it. Subsequent images were consecutively evaluated in the follow-up mode to ensure spatial reliability. In multimodal comparisons, landmarks such as vessel bifurcations were used for localization and alignment.

RESULTS

• **COHORT CHARACTERISTICS:** Thirty-six eyes of 18 genetically confirmed MIDD patients (11 females, 7 males) were evaluated in the study (Table). The mean age (±SD,

years) was 53.4 ± 11.6 (range, 22.4-71.6), the mean age of onset (ie, first reported appearance of visual symptoms or retinal alterations) of 47.3 ± 8.4 years (range, 21.0-62.0), and the mean retinal disease duration was 6.1 ± 6.2 years (range, 0.0-20.7) at baseline (ie, first recorded visit with OCT imaging). The age of onset appeared to describe a Gaussian distribution with one outlier that was extensively reported before,[5] who showed subjective symptoms significantly earlier (21.0 years) than the other patients (≥38.5 years). All MIDD patients had been diagnosed with diabetes mellitus. However, only 4 eyes of 2 patients revealed diabetic retinopathy (graded as mild nonproliferative diabetic retinopathy). Cataract or pseudophakia was reported in all patients older than 50 years (not specified in more detail in the records). Two patients were described with cardiovascular complications (cardiomyopathy), 2 eyes with glaucoma, and 1 eye with Fuchs endothelial dystrophy.

• **RORA AT BASELINE:** At baseline, 3 eyes of 2 patients did not show any area of RORA (Figure 1, A). Both patients were among the youngest included subjects (22.4 and 50.5 years of age). The other 33 eyes revealed atrophic patches, mostly in a circular distribution around the fovea between 5 and 15° eccentricity (Figure 1, B). If the area of RORA exceeded approximately 12 mm^2, it has been ascertained to extend into the central 5°. Eight eyes presented with fovea-involving RORA at baseline, which was associated in the majority (7 eyes) with a best-corrected visual acuity of <1.0 logarithm of the minimum angle of resolution (LogMAR) (>20/200 Snellen equivalent). As previously reported,[5] the size of atrophy was very variable in MIDD. It ranged from 0.06 to 86.91 mm^2 in the present cohort (Table). Peripapillary atrophy was a quite common finding and present to some extent in 28 eyes of 14 patients. Peripapillary atrophy was not confluent with the macular RORA except in the 3 eyes with the most extensive atrophic changes. In this subgroup, some form of delineation was identified that was characterized by an interrupted line of apparently partly preserved outer retinal layers in OCT (Figure 1, C).

• **PRE-RORA FEATURES:** Over the observation period of 4.6 ± 2.8 years (range, 0.5-8.5 years), a variety of OCT features were identified that were particularly found to signify high risk of progression to RORA. In the following, we describe outer retinal abnormalities such as external limiting membrane (ELM) and ellipsoid zone (EZ) disruption, subretinal deposits, hypertransmission of the OCT signal into the choroid and sclera, outer retinal layer thinning associated with subsidence of inner retinal layers, hyporeflective wedges, outer retinal tubulations, or subretinal hyperreflective lesion.

EZ and ELM integrity loss and subretinal deposits. EZ and ELM represent hyperreflective bands in the outer retina. In our cohort, the loss of EZ was the first sign of RORA development and usually associated with subretinal deposits between Bruch membrane and retinal pigment epithelium that resemble cuticular drusen. The subretinal deposits usually showed overlying retinal pigment epithelium as a hyperreflective cap and homogenous internal structure of medium-low reflectivity. They were associated with hyperreflective dots in IR image and hyperautofluorescent dots in AF imaging. The course showed reflectivity changes in the overlaying OCT layers leading to loss of a delimitable ELM (Figure 2).

Retinal pigment epithelial integrity loss and hypertransmission of the OCT signal. The retinal pigment epithelium displays as the most external hyperreflective OCT layer.[13] Vanishing subretinal deposits led to a spatially related retinal pigment epithelial signal discontinuation that was associated with hypertransmission of the OCT signal into the choroid and loss of AF intensity (Figure 2). Both retinal pigment epithelial loss and hypertransmission are part of the definition of RORA[11] and were therefore found in the area of RORA. However, they were also found in some transient states (ie, areas of retinal pigment epithelial disruption with preserved but partly abnormal outer nuclear layer [ONL]; Figure 3).

Intraretinal hyperreflective foci and microcystoid lesions. Intraretinal hyperreflective foci and microcystoid lesions are characterized as circumscribed lesions that show at least the reflectivity of the retinal pigment epithelium and no to low reflectivity, respectively. They could occasionally be observed in the obtained images. If present, they were located in the ONL and/or outer plexiform layer (OPL) in association with incomplete RORA (ie, subretinal deposits, EZ loss, retinal pigment epithelial loss, or hypertransmission; Figure 2).

ONL thinning and photoreceptor outer segment shortening. ONL thinning associated with subsidence of inner retinal layers as well as photoreceptor outer segment shortening had been described in nascent GA secondary to AMD corresponding with the termination of an intact retinal pigment epithelial layer.[14,15] In the qualitative assessment of OCT B-scans, ONL thinning and photoreceptor outer segment shortening was difficult to identify. In general, ONL thickness seemed preserved for long time in atrophy development. In some cases of our cohort, normal ONL thickness was observed even in the presence of retinal pigment epithelial loss and EZ loss, explaining findings like relatively good visual acuity in the presence of fovea-involving retinal pigment epithelial atrophy (Figure 3).[5] However, the reflectivity of the outer retinal layers seemed to be irregular in these cases (Figure 2). Loss of ONL and photoreceptor outer segment was observed in the center of the atrophic areas (ie, central to hyporeflective wedges).

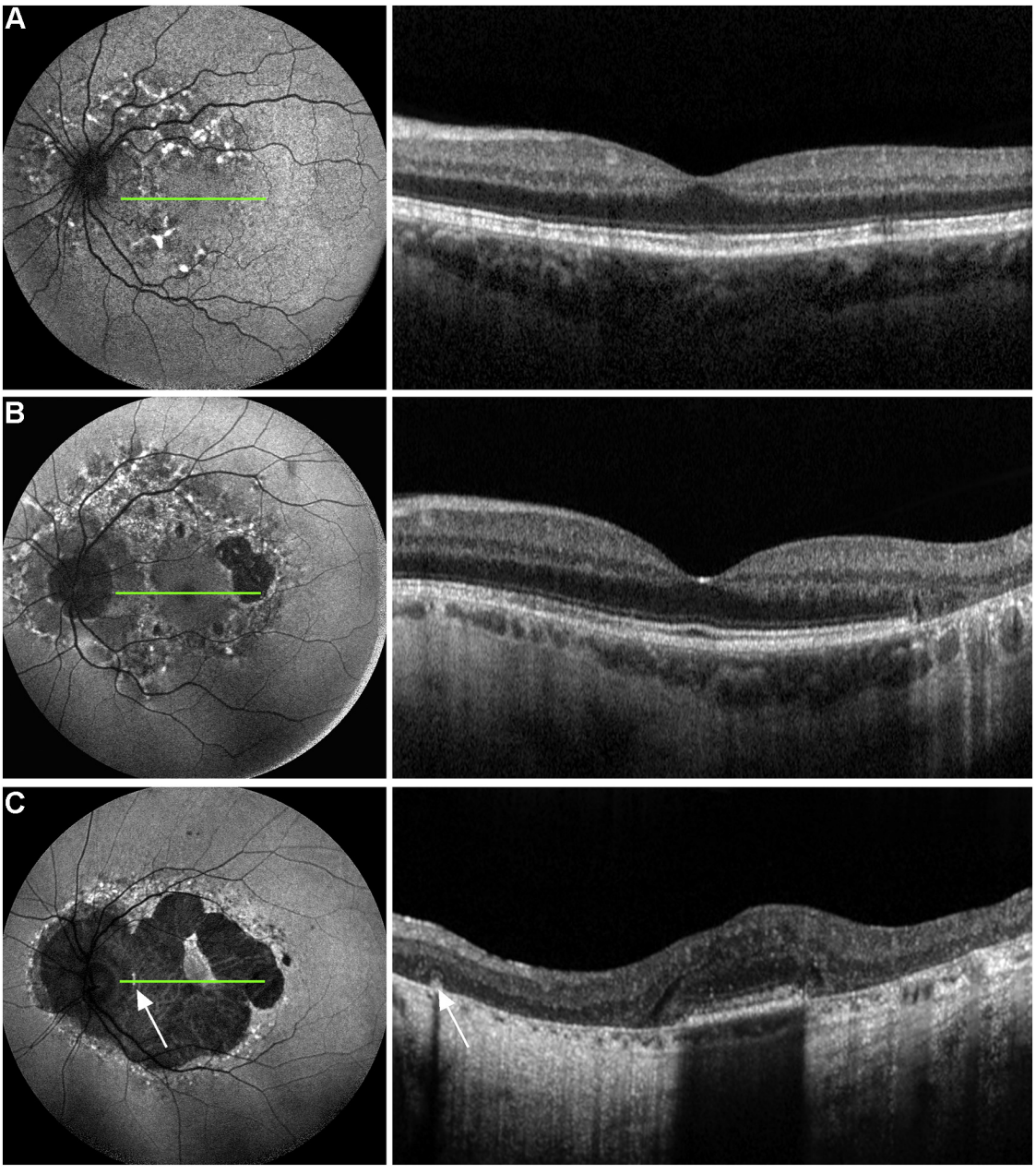

FIGURE 1. Presentation of retinal pigment epithelial (RPE) and outer retinal atrophy (RORA). Exemplary fundus autofluorescence (left) and associated optical coherence tomography (OCT, right) images of different patients demonstrate the variable manifestation of RORA. The green line indicates the approximate location of the respective OCT scan. A. At baseline, a minority showed no area of RORA in our cohort. B. Most patients revealed multiple spots of RORA in a circular area around the fovea between 5- and 15-degrees eccentricity associated with other qualitative alterations (hyperautofluorescent spots) in between. C. In cases of widespread RORA, it is extended into the central 5°. Whenever RORA coalesced with peripapillary atrophy, a separation line could be identified in the fundus autofluorescent images associated with partly preserved but altered outer retinal layers or evolving outer retinal tubulations in OCT (white arrow).

Hyporeflective wedges. Hyporeflective wedges describe a triangular, hyporeflective structure at the border of RORA that is based on Bruch membrane and extending to the inner limit of the OPL. At the margin of most RORA spots larger than 0.2 mm^2, hyporeflective wedges were detected in our cohort. It was located within the area of retinal pigment epithelial loss and hypertransmission. Similar to the original description in GA secondary to AMD,[16] a distinct hyperreflective separation between this OCT feature and the end of ONL was generally present. With progression of the RORA, the hyporeflective wedges moved correspondingly (Figure 2).

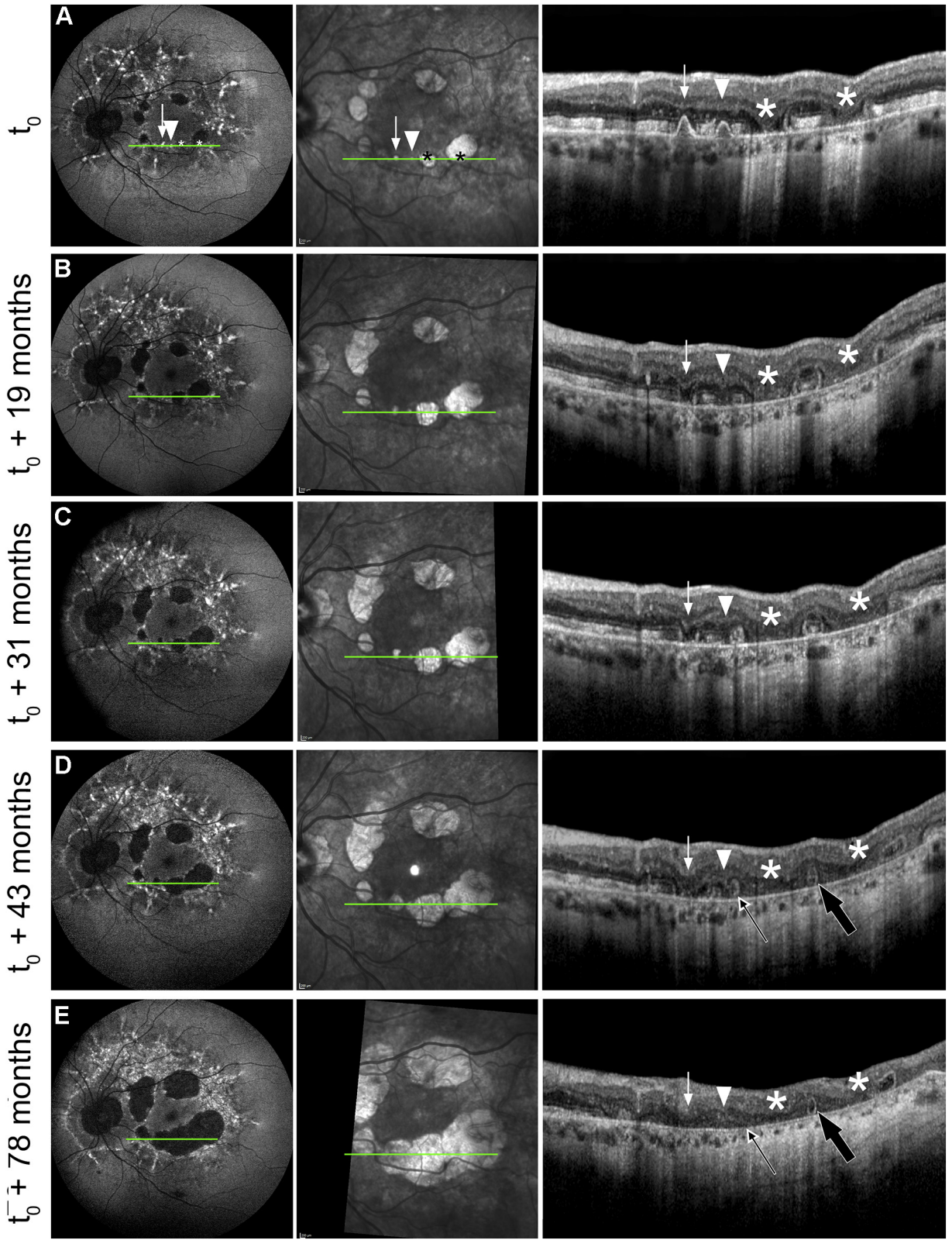

FIGURE 2. Development and progression of retinal pigment epithelial (RPE) and outer retinal atrophy (RORA). Serial fundus autofluorescence (AF, left), infrared reflectance (IR, middle), and associated optical coherence tomography (OCT, right) images of an exemplary eye that demonstrated the different stages to and the progression of RORA. The green line indicates the approximate location of the respective OCT scan. A. As a first sign of RORA development, subretinal deposits can be found that show homogenous internal medium-low reflectivity as well as overlying elevated retinal pigment epithelium, and are associated with EZ loss (arrowhead)

Outer retinal tubulations. Outer retinal tubulations (ORTs) appear as oval hyporeflective structures surrounded by hyperreflective margins on OCT scans. In our cohort, ORTs were frequently found within the areas of retinal pigment epithelial atrophy directly adjacent to Bruch membrane reaching into the OPL. In the longitudinal evaluation, they developed in the margin region when individual atrophic spots coalesced and were associated with hyporeflective wedges. Over the observation time, the ORTs often disappeared, while RORA expanded onto this area (Figure 2).

Subretinal hyperreflective lesion. In the whole observation time, subretinal fluid was only observed in the exceptional patient with early disease onset (Figure 4). In one eye, it resorbed over time and did not progress to RORA. In the second eye, a thickened hyperreflective band was found external to the EZ and with rough borders to the subretinal fluid. In the first visit, the hyperreflective mound appeared as a hyperautofluorescent lesion on AF images, resembling vitelliform lesions. In the follow-up, there was a loss of subretinal fluid as well as loss of retinal pigment epithelium, EZ and ELM. Therefore, the hyperreflective material was directly adjacent to the ONL. The reabsorption of this material was followed by a loss of ONL in the original area of the subretinal fluid completing the definition of RORA. No ORTs could be found in these eyes (Figure 4).

DISCUSSION

THIS IS THE FIRST STUDY TO SYSTEMATICALLY INVESTIGATE structural features associated with development and progression of RORA secondary to a monogenetic mitochondrial disorder. As RORA in MIDD had been shown to be delineable, traceable, and allows to monitor disease progression,[5] the findings of this study might allow for further insights into the pathomechanisms of retinopathies secondary to mitochondrial disorders and for future validation of novel susceptible surrogate markers for disease progression and possible therapeutic effects at earlier disease stages.

The presented findings provided evidence for a consistent sequence of OCT features from earlier disease stages to the end stage of RORA (Figure 5): (1) Loss of EZ appeared first associated with subretinal deposit, as well as hyperreflective foci and microcystoid lesions in some cases. (2) Additional loss of ELM then happened with increasing reflectivity changes of the ONL. (3) In the next step, loss of retinal pigment epithelium could be observed that was associated with hypertransmission of OCT signal into the choroid. From this stage onward, the subretinal deposits were absent. (4) With loss of the ONL, the definition of RORA was completed. Areas of RORA were usually bordered by hyporeflective wedges and more externally ELM and EZ loss. (5) With progression of RORA, EZ loss was the most widespread observed OCT alteration (congruent with the presented development of RORA). It might therefore be described as "leading disease front" for OCT features in MIDD, in analogy to changes in near-infrared AF in Stargardt disease as proposed by Cideciyan and collegues.[17] (6) Whenever 2 areas of RORA or lobed areas of RORA coalesced, there was the possibility to develop ORTs at the location of the last preserved outer retinal layers.

For some of the described OCT features, the histopathologic correlate has not been fully described. Although ELM is generally thought to correspond to junctional complexes between photoreceptors and Müller cells,[18] EZ origin is still disputed: it originally had been thought to represent the junction between the photoreceptor inner and outer segments and named the IS-OS junction. Because of its correspondence to the photoreceptor inner segment ellipsoid, it was later renamed.[19] As part of the inner segment, ellipsoids are characterized by a high density of mitochondria.[18] Therefore, a presumed mitochondriopathy would be expected to affect this structure first, which was confirmed in this study. Nevertheless, we can only hypothesize why the primary presentation of EZ loss is focal at a circumscribed area rather than diffuse in MIDD. The heteroplasmy found in patients with mitochondriopathies (ie, a varying coexpression of inherited polymorphisms and somatic pathology within individual mitochondrial genomes)[20] might partly explain this finding. Furthermore, recent adaptive optics studies have questioned this origin, and EZ might be too thick and proximally located to be generated by the ellipsoids of the inner segments.[21] However, only foveal cones had been imaged in that study, which may explain the inconsistency with earlier reports. The subretinal deposits usually showed a hyperreflective cap that most likely represents the retinal pigment epithelium similar to drusen in AMD.[22] They usually revealed a

as well as, partly, ELM loss (arrow). They were associated with hyperreflectivity in IR and hyperautofluorescent spots in AF. In the demonstrated OCT B-scan, 2 separate areas of RORA are also present bordered by hyporeflective wedges. B. After 19 months, the subretinal deposits have been vanished (arrow and arrowhead), leaving behind an area with loss of ELM, EZ, and retinal pigment epithelium associated with hypertransmission of OCT signal into the choroid. Despite reflectivity changes, ONL thickness seemed to be preserved. C and D. For the following visit, a thinning of the ONL in the respective areas could be observed (C), until they could be also defined as RORA and revealed hyporeflective wedges at their border (D). With exceeding RORA areas, 3 areas coalesced leaving outer retinal tubulations (ORTs) at the former shoreline behind (open arrows). E. In the further observation time, one ORT vanished (narrow open arrow), whereas the other stayed present but seemed to regress (broad open arrow).

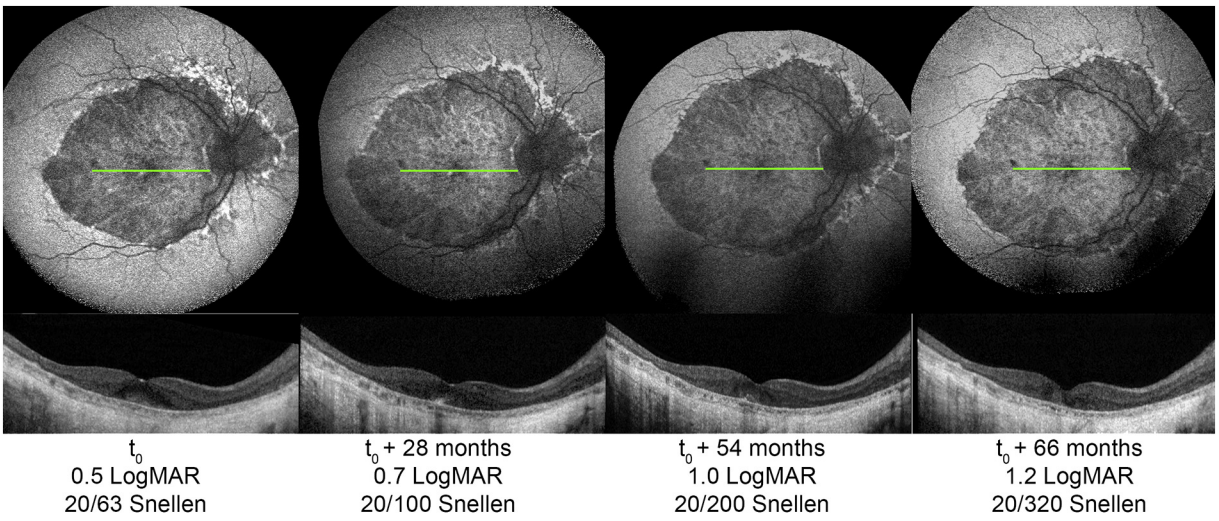

FIGURE 3. Visual acuity at development of foveal retinal pigment epithelial (RPE) and outer retinal atrophy (RORA). Serial fundus autofluorescence (first row) and associated optical coherence tomography (OCT, second row) images of an exemplary eye that demonstrated preserved visual acuity despite fovea-involving retinal pigment epithelial atrophy (first column). The ONL thinning seems delayed compared with loss of retinal pigment epithelium, external limiting membrane (ELM), and ellipsoid zone (EZ). Loss of visual acuity was associated with progression of ONL reflectivity alterations and thinning (second to last column). The green line indicates the approximate location of the respective OCT scan.

homogenous internal structure of medium-low reflectivity. In AMD, the hyporeflective core of drusen is thought to correspond to crystalline hydroxyapatite nodules.[23] As subretinal deposits in MIDD vanish in association with development of RORA, similar to that described in AMD,[22] a related composition might be hypothesized. Concerning the vitelliform-like lesion found in one eye, a variety of different conditions have been described to be associated with acquired vitelliform lesions.[24] The material is thought to originate from shed photoreceptor material that accumulates because of dysfunctional retinal pigment epithelium, pigment-containing retinal pigment epithelial cells, expelled retinal pigment epithelial organelles, and macrophages that migrate into the subretinal space.[25] Given the presentation of the hyperreflective material in the outer retina and the obvious retinal pigment epithelial layer disruption early in the follow-up (Figure 4), outer segment shedding associated with impaired disc clearance due to presumed retinal pigment epithelial phagocytosis defect might indeed be a possible explanation. Intraretinal hyperreflective foci might represent retinal pigment epithelial cells or microglia as they show at least the reflectivity of the retinal pigment epithelium, similar to descriptions in AMD.[26,27] Also similar to AMD, microcystoid changes in MIDD have been seen in the ONL, in contrast to optic neuropathies that can be associated with mitochondriopathies where these changes would be expected in the inner retinal layers.[28] The ONL is thought to derive from the photoreceptor cell bodies.[29] As ONL thinning and loss of visual acuity was delayed compared with the development of loss of retinal pigment epithelium and associated hypertransmission of OCT signal into the choroid, it may be hypothesized that photoreceptors survive longer than the retinal pigment epithelium in the development and progression of RORA. A similar interpretation has been hypothesized in a previous AF study.[5] However, reflectivity changes within the respective layer and some degree of impaired visual acuity could be found at disease stage III indicating beginning alterations in the photoreceptor microstructure. Hyporeflective wedges are thought to derive from axonal swelling or interaxonal edema within the OPL.[16] This might also explain the location within this layer and the separation between hyporeflective wedges and ONL as consistently observed. Finally, ORTs have been described in various degenerative retinal diseases including 3 cases of MIDD. Apart from OCT B-scans, they are reported to appear as straight or branching tubules on OCT C-scans.[30–32] Because of its limited location over retinal pigment epithelial atrophy or fibrosis as well as association to OPL subsidence sign, ORTs are thought to derive from degenerating photoreceptors.[33] Our observations of ORT development in the last remaining island when areas of RORA coalesced, and the diminishing or vanishing of ORTs in its further progression, support this hypothesis.

The described OCT features in MIDD differ from typical findings in diabetic retinopathy, which was absent in the majority of our cohort despite the long interval since the establishment of a diagnosis of diabetes. In contrast, there were distinct similarities between RORA development in MIDD and described features in nascent GA secondary to AMD, the leading cause of blindness in the industrialized

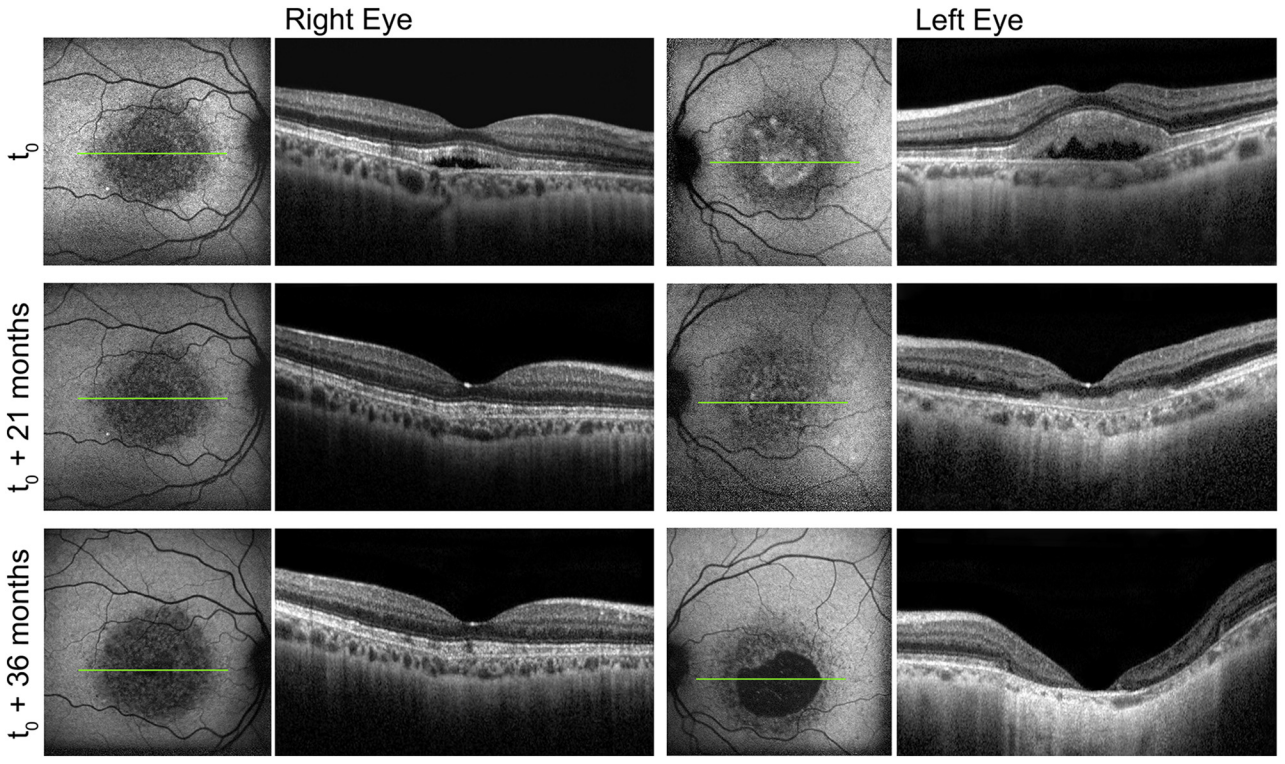

FIGURE 4. Development of retinal pigment epithelial (RPE) and outer retinal atrophy (RORA) following vitelliform-like hyperreflective lesion. The fundus autofluorescence and associated optical coherence tomography (OCT) images of the exceptional subject, which revealed subretinal fluid in both eyes at baseline (t_0), are demonstrated. The green line indicates the approximate location of the respective OCT scan. In the right eye (left), the outer retinal layers seemed to be of quite regular configuration despite the splitting (first row). After reabsorption (second to last row), the retinal layers kept relatively preserved. In the left eye (right), the area of the subretinal fluid was hyperautofluorescent and revealed thickened hyperreflective material at the level of the photoreceptor outer segments (first row). Over the observation time, the lesion progressed to RORA (second to last row).

world.[11] As the most practical approach to studies and interventional trials that target specific pathogenic pathways in AMD is to evaluate these strategies first in a model disease, and, if proven, then moving to a proof of concept AMD trial, MIDD would be a perfect model disease for mitochondrial dysfunction that also has been implicated in the pathogenesis of AMD.[34] The evaluation of a pure pathophysiologic pathway might further allow for conclusions concerning the composition of underlying pathways in AMD. However, caution has to be applied because of concomitant diseases or medications that could affect disease progression rates, as well as the heteroplasmy in MIDD: disease-specific features are very variable, and the complexity of determining a robust endpoint for nonocular features is difficult.

Retinal disease manifestations is defined by pattern dystrophy-like alterations and RORA.[4,35] Because of the typical distribution of these retinal alterations at 5 to 15° eccentricity (Figure 1),[4] visual acuity does also not constitute a useful endpoint as it usually stays stable over the observation time. Most interventional and observational studies for retinopathies that develop RORA in disease progression have assessed the progression of RORA as primary structural study endpoint.[5,8,9,36] For MIDD, a recent study demonstrated that a clinical trial using reduction in RORA enlargement in MIDD may allow for a clean proof-of-concept clinical trial endpoint with a manageable sample size.[5] However, most of these studies including the latter relied on short-wavelength AF imaging, which is in particular more prone to artifacts and loss of image quality due to media opacity compared to OCT imaging.[37,38] As all patients above a certain age threshold in our cohort presented either cataract or pseudophakia (earlier than you would expect in general population),[39,40] lens status and imaging technology should be considered for clinical trial design when dealing with MIDD, even if it is unlikely in the industrialized world that cataract surgery will be postponed until it interferes with imaging. Furthermore, it is possible that the most effective upcoming therapeutic approach might be directed to earlier disease stages before a potential point of no return is reached.[10,38,41] Early OCT features prior to RORA (as presented in this study) might therefore constitute appropriate study end points. However, the difficulty of evaluating transient alterations has been shown in AMD where the role of drusen volume as a

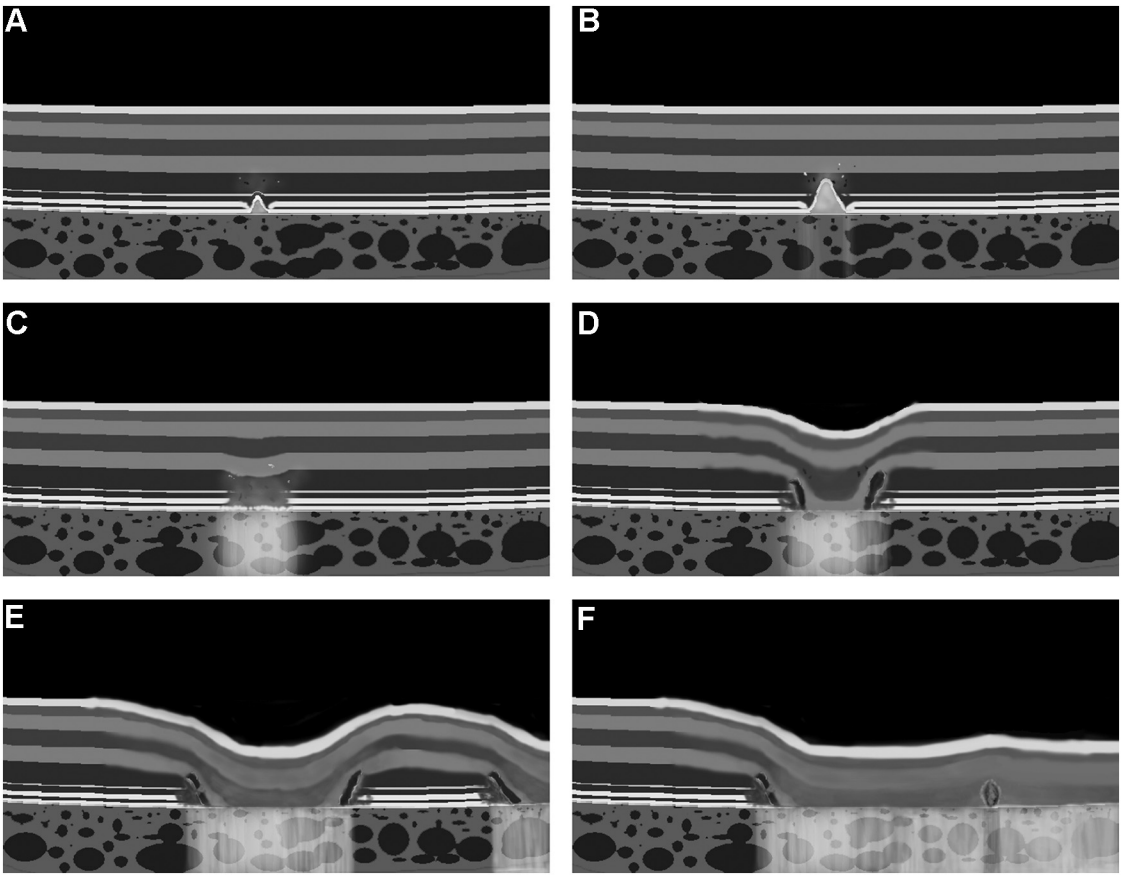

FIGURE 5. Schematic development and progression of retinal pigment epithelial (RPE) and outer retinal atrophy (RORA). Based on the findings, the schematic model demonstrates the development and progression of RORA in optical coherence tomography (OCT) images. A. The first observed alteration was the loss of the ellipsoid zone (EZ) integrity associated with subretinal deposits showing homogenous medium-low reflectivity as well as overlying elevated retinal pigment epithelium, and change of outer nuclear layer (ONL) reflectivity. B. This was followed by a loss of external limiting membrane (ELM) integrity, in some scans associated with intraretinal hyperreflective foci and microcystoid lesions. C. Vanishing subretinal deposits was followed by loss of retinal pigment epithelial integrity, which led to hypertransmission of the OCT signal into the choroid. In this stage, the ONL thickness seemed preserved, whereas reflectivity changes progressed. D. With further loss of ONL, full RORA was present, bordered by hyporeflective wedges and, more eccentrically, EZ loss. E. In progression of the RORA, these alterations moved centrifugally in the same sequence. F. When 2 areas of RORA coalesced, outer retinal tubulations could occasionally be observed.

predictor of GA development is not completely solved. Greater drusen volume as well as retinal pigment epithelial drusen complex thinning predicts progression to GA.[42,43] Furthermore, it was beyond the scope of this study to evaluate the reliability of the identification, the accuracy as predictive factors, or the relative RORA conversion rate for each described feature. These evaluations are prerequisites to designing a study protocol that relies on these OCT features and to justify a significant reduction of the sample size for future interventional trials, which is important given the rarity of MIDD. Prospective studies focusing on these aspects are therefore required, as has been done for AMD.[44,45] Here, a related lexicon developed by the CAM group that describes RORA and preceding OCT features has already been implemented by reading centers for current and upcoming observational and interventional trials.[11,46,47] The LEAD study is a prominent example[47]: although the study intervention did not show a benefit, the LEAD study illustrated the possibility to effectively design an interventional study based on imaging features representing early disease stages before the development of RORA as part of a combined endpoint.

Machine learning application offers a great potential in screening, differential diagnostics, and identification of disease progression or treatment effects.[48] Imaging, especially OCT imaging, is indispensable to the modern retina specialist[49] and lends to artificial intelligence approaches. Artificial intelligence approaches have recently been used to identify and classify imaging features that are known to represent risk factors for RORA secondary to AMD. Hyper-reflective foci, hyporeflective foci within drusen, subretinal drusenoid deposits, or outer retinal thinning

have been analyzed. Machine learning tools have been presented to identify OCT features with an area under the curve of 0.94 to 0.99, sensitivity of 0.90 to 1.00, and specificity of 0.89 to 0.92.[12,45] The present study identified additional features for the development and progression of RORA in MIDD, such as vitelliform-like shedding dome, hypertransmission of OCT signal into choroid, loss of ELM, loss of EZ, loss of retinal pigment epithelium, ONL reflectivity changes, and hyporeflective wedges. As we revealed evidence of the conversion to RORA and these features are present in a multitude of other retinopathies, it might be worth evaluating the accuracy of the identification of these features by machine learning algorithms in the future.

Retinal imaging experts identified and interpreted the presented OCT features. As the image feature descriptions were based on retrospective data, the number of visits, the interval, and the quality of images differed between and within the patients. The interpretation of OCT findings happened to our knowledge and available data of previous studies on retinal diseases and histopathologic correlations as presented above. It cannot be excluded that features have been missed and other data sets could provide addition conclusions. However, the uniformity of the presence and sequence of the described imaging features (Figure 5) has the potential to provide the framework for further prospective studies that assess the pathophysiology and disease progression of retinopathy secondary to MIDD.

In summary, this study demonstrated that RORA develops in a consistent sequence characterized by particular OCT features in MIDD patients. This might not only provide further insights into the pathomechanisms of retinopathies secondary to mitochondrial disorder but also allow to potentially define novel surrogate markers for disease progression and possible therapeutic effects in upcoming trials. As mitochondrial dysfunction also has been implicated in the pathogenesis of more common multifactorial retinal conditions like AMD, such a proposed disease model can represent an efficient methodology to evaluate disease manifestation and determine effects of therapeutic interventions.

FUNDING/SUPPORT: THIS WORK WAS SUPPORTED BY THE GERMAN RESEARCH FOUNDATION (GRANT MU4279/2-1 TO PLM), THE United Kingdom's National Institute for Health Research of Health's Biomedical Research Centre for Ophthalmology at Moorfields Eye Hospital and UCL Institute of Ophthalmology. The views expressed are those of the authors, not necessarily those of the Department of Health. The funder had no role in study design, data collection, analysis, or interpretation, or the writing of the report. Financial Disclosures: The authors indicate no financial support or conflicts of interest. All authors attest that they meet the current ICMJE criteria for authorship.

REFERENCES

1. Reardon W, Ross RJ, Sweeney MG, et al. Diabetes mellitus associated with a pathogenic point mutation in mitochondrial DNA. *Lancet* 1992;340(8832):1376–1379.
2. 't Hart LM, Jansen JJ, Lemkes HHPJ, de Knijff P, Maassen JA. Heteroplasmy levels of a mitochondrial gene mutation associated with diabetes mellitus decrease in leucocyte DNA upon aging. *Hum Mutat* 1996;7(3):193–197.
3. Naing A, Kenchaiah M, Krishnan B, et al. Maternally inherited diabetes and deafness (MIDD): diagnosis and management. *J Diabetes Complications* 2014;28(4):542–546.
4. Massin P, Virally-Monod M, Vialettes B, et al. Prevalence of macular pattern dystrophy in maternally inherited diabetes and deafness. GEDIAM Group. *Ophthalmology* 1999;106(9):1821–1827.
5. Müller PL, Treis T, Pfau M, et al. Progression of retinopathy secondary to maternally inherited diabetes and deafness—evaluation of predicting parameters. *Am J Ophthalmol* 2020;213:134–144.
6. Viscomi C, Bottani E, Zeviani M. Emerging concepts in the therapy of mitochondrial disease. *Biochim Biophys Acta* 2015;1847(6-7):544–557.
7. Finger RP, Fimmers R, Holz FG, Scholl HPN. Prevalence and causes of registered blindness in the largest federal state of Germany. *Br J Ophthalmol* 2011;95(8):1061–1067.
8. Csaky KG, Richman EA, Ferris FL. Report from the NEI/FDA Ophthalmic Clinical Trial Design and Endpoints Symposium. *Invest Ophthalmol Vis Sci* 2008;49(2):479–489.
9. Holz FG, Strauss EC, Schmitz-Valckenberg S, van Lookeren Campagne M. Geographic atrophy: clinical features and potential therapeutic approaches. *Ophthalmology* 2014;121(5):1079–1091.
10. Schaal KB, Rosenfeld PJ, Gregori G, Yehoshua Z, Feuer WJ. Anatomic clinical trial endpoints for nonexudative age-related macular degeneration. *Ophthalmology* 2016;123(5):1060–1079.
11. Sadda SR, Guymer R, Holz FG, et al. Consensus definition for atrophy associated with age-related macular degeneration on OCT: classification of atrophy report 3. *Ophthalmology* 2018;125(4):537–548.
12. Wintergerst MWM, Schultz T, Birtel J, et al. Algorithms for the automated analysis of age-related macular degeneration biomarkers on optical coherence tomography: a systematic review. *Transl Vis Sci Technol* 2017;6(4):10.
13. Spaide RF, Curcio CA. Anatomical correlates to the bands seen in the outer retina by optical coherence tomography: literature review and model. *Retina* 2011;31(8):1609–1619.
14. Dolz-Marco R, Balaratnasingam C, Messinger JD, et al. The border of macular atrophy in age-related macular degeneration: a clinicopathologic correlation. *Am J Ophthalmol* 2018;193:166–177.
15. Zanzottera EC, Ach T, Huisingh C, Messinger JD, Spaide RF, Curcio CA. Visualizing retinal pigment epithelium phenotypes in the transition to geographic atrophy in age-related macular degeneration. *Retina* 2016;36(Suppl 1):S12–S25.
16. Monés J, Biarnés M, Trindade F. Hyporeflective wedge-shaped band in geographic atrophy secondary to age-related

macular degeneration: an underreported finding. *Ophthalmology* 2012;119(7):1412–1419.
17. Cideciyan AV, Swider M, Schwartz SB, Stone EM, Jacobson SG. Predicting progression of ABCA4-associated retinal degenerations based on longitudinal measurements of the leading disease front. *Invest Ophthalmol Vis Sci* 2015; 56(10):5946–5955.
18. Xie W, Zhao M, Tsai SH, et al. Correlation of spectral domain optical coherence tomography with histology and electron microscopy in the porcine retina. *Exp Eye Res* 2018;177:181–190.
19. Litts KM, Zhang Y, Bailey Freund K, Curcio CA, Freund KB, Curcio CA. Optical coherence tomography and histology of age-related macular degeneration support mitochondria as reflectivity sources. *Retina* 2018;38(3):445–461.
20. Stefano GB, Bjenning C, Wang F, Wang N, Kream RM. Mitochondrial heteroplasmy. *Adv Exp Med Biol* 2017;982: 577–594.
21. Tao LW, Wu Z, Guymer RH, Luu CD. Ellipsoid zone on optical coherence tomography: a review. *Clin Exp Ophthalmol* 2016;44(5):422–430.
22. Balaratnasingam C, Cherepanoff S, Dolz-Marco R, et al. Cuticular drusen: clinical phenotypes and natural history defined using multimodal imaging. *Ophthalmology* 2018; 125(1):100–118.
23. Tan ACS, Pilgrim MG, Fearn S, et al. Calcified nodules in retinal drusen are associated with disease progression in age-related macular degeneration. *Sci Transl Med* 2018; 10(466).
24. Freund KB, Laud K, Lima LH, Spaide RF, Zweifel S, Yannuzzi LA. Acquired vitelliform lesions: correlation of clinical findings and multiple imaging analyses. *Retina* 2011; 31(1):13–25.
25. Chen KC, Jung JJ, Curcio CA, et al. Intraretinal hyperreflective foci in acquired vitelliform lesions of the macula: clinical and histologic study. *Am J Ophthalmol* 2016;164: 89–98.
26. Nassisi M, Fan W, Shi Y, et al. Quantity of intraretinal hyperreflective foci in patients with intermediate age-related macular degeneration correlates with 1-year progression. *Invest Ophthalmol Vis Sci* 2018;59(8):3431.
27. Balaratnasingam C, Messinger JD, Sloan KR, Yannuzzi LA, Freund KB, Curcio CA. Histologic and optical coherence tomographic correlates in drusenoid pigment epithelium detachment in age-related macular degeneration. *Ophthalmology* 2017;124(5):644–656.
28. Carbonelli M, La Morgia C, Savini G, et al. Macular microcysts in mitochondrial optic neuropathies: prevalence and retinal layer thickness measurements. *PLoS One* 2015; 10(6):e0127906.
29. Lujan BJ, Roorda A, Croskrey JA, et al. Directional optical coherence tomography provides accurate outer nuclear layer and Henle fiber layer measurements. *Retina* 2015;35(8): 1511–1520.
30. Zweifel SA, Engelbert M, Laud K, Margolis R, Spaide RF, Freund KB. Outer retinal tubulation a novel optical coherence tomography finding. *Arch Ophthalmol* 2009;127(12): 1596–1602.
31. Tripathy K, Sarma B, Mazumdar S. Outer retinal tubulation and inner retinal pseudocysts in a patient with maternally inherited diabetes and deafness evaluated with optical coherence tomography angiogram. *Indian J Ophthalmol* 2020;68(1): 250–253.
32. Raja MS, Goldsmith C, Burton BJL. Outer retinal tubulations in maternally inherited diabetes and deafness (MIDD)-associated macular dystrophy. *Graefes Arch Clin Exp Ophthalmol* 2013;251(9):2265–2267.
33. Preti RC, Govetto A, Filho RGA, et al. Optical coherence tomography analysis of outer retinal tubulations: sequential evolution and pathophysiological insights. *Retina* 2018; 38(8):1518–1525.
34. Suter M, Remé C, Grimm C, et al. Age-related macular degeneration. The lipofusion component *N*-retinyl-*N*-retinylidene ethanolamine detaches proapoptotic proteins from mitochondria and induces apoptosis in mammalian retinal pigment epithelial cells. *J Biol Chem* 2000;275(50): 39625–39630.
35. Daruich A, Matet A, Borruat F-X. Macular dystrophy associated with the mitochondrial DNA A3243G mutation: pericentral pigment deposits or atrophy? Report of two cases and review of the literature. *BMC Ophthalmol* 2014;14:77.
36.. Müller PL, Pfau M, Treis T, et al. Progression of abca4-related retinopathy—prognostic value of demographic, functional, genetic, and imaging parameters. *Retina* 2020;1–14. https://doi.org/10.1097/IAE.0000000000002747.
37. Müller PL, Pfau M, Mauschitz MM, et al. Comparison of green versus blue fundus autofluorescence in abca4-related retinopathy. *Transl Vis Sci Technol* 2018;7(5):13.
38. Müller PL, Birtel J, Herrmann P, Holz FG, Charbel Issa P, Gliem M. Functional relevance and structural correlates of near infrared and short wavelength fundus autofluorescence imaging in ABCA4-related retinopathy. *Transl Vis Sci Technol* 2019;8(6):46.
39. Kanthan GL, Wang JJ, Rochtchina E, et al. Ten-year incidence of age-related cataract and cataract surgery in an older Australian population. *Ophthalmology* 2008;115(5): 808–814.e1.
40. Klein BEK, Klein R, Lee KE. Incidence of age-related cataract over a 10-year interval: the Beaver Dam Eye Study. *Ophthalmology* 2002;109(11):2052–2057.
41.. Müller PL, Dysli C, Hess K, Holz FG, Herrmann P. Spectral fundus autofluorescence excitation and emission in abca4-related retinopathy. *Retina* 2019;1–11. https://doi.org/10.1097/IAE.0000000000002726.
42. Folgar FA, Yuan EL, Sevilla MB, et al. Drusen volume and retinal pigment epithelium abnormal thinning volume predict 2-year progression of age-related macular degeneration. *Ophthalmology* 2016;123:39–50.e1.
43. De Amorim Garcia Filho CA, Yehoshua Z, Gregori G, et al. Change in drusen volume as a novel clinical trial endpoint for the study of complement inhibition in age-related macular degeneration. *Ophthalmic Surg Lasers Imaging Retina* 2014; 45:18–31.
44. Sleiman K, Veerappan M, Winter KP, et al. Optical coherence tomography predictors of risk for progression to non-neovascular atrophic age-related macular degeneration. *Ophthalmology* 2017;124(12):1764–1777.
45. Saha S, Nassisi M, Wang M, et al. Automated detection and classification of early AMD biomarkers using deep learning. *Sci Rep* 2019;9(1):10990.
46. Holz FG, Sadda SR, Staurenghi G, et al. Imaging protocols in clinical studies in advanced age-related macular

degeneration: recommendations from classification of atrophy consensus meetings. *Ophthalmology* 2017;124(4):464–478.
47. Guymer RH, Wu Z, Hodgson LAB, et al. Subthreshold nanosecond laser intervention in age-related macular degeneration: the LEAD randomized controlled clinical trial. *Ophthalmology* 2019;126(6):829–838.
48. Liu X, Faes L, Kale AU, et al. A comparison of deep learning performance against health-care professionals in detecting diseases from medical imaging: a systematic review and meta-analysis. *Lancet Digit Heal* 2019;1(6):e271–e297.
49. Fujimoto J, Swanson E. The development, commercialization, and impact of optical coherence tomography. *Invest Opthalmol Vis Sci* 2016;57(9):OCT1–OCT13.